DE GRUYTER OPEN

Archives of Hydro-Engineering and Environmental Mechanics
Vol. 65 (2018), No. 4, pp. 255–275
DOI: 10.1515/heem-2018-0016

Transport of Fine Sediments in Marine Waterbodies Near River Mouths: Preliminary Results *

Grzegorz R. Cerkowniak[1], Marek Kowalewski[2]

[1]Institute of Hydro-Engineering, Polish Academy of Sciences, 7 Kościerska, 80-328 Gdańsk, Poland, Corresponding author, e-mail: grzegorz.cerkowniak@ibwpan.gda.pl; [2]Institute of Oceanography, University of Gdańsk, al. Marszałka Piłsudskiego 46, 81-378 Gdynia, Poland, e-mail: ocemk@ug.edu.pl

(Received November 02, 2018; revised December 28, 2018)

Abstract

Transport of fine sediments depends mainly on the efficiency of flocculation. Flocculation, understood as the result of simultaneous processes of aggregation of particles and floc break-up, is a common phenomenon in marine environments. It is typical of fine sediments. This study presents a mathematical model of fine sediment transport. A model of flocculation is an important part of this model. Its main assumption is that flocculation is governed by turbulence. The model was qualitatively tested in a simplified theoretical waterbody. Such factors as the wind direction, wind speed, river discharge and concentration of suspension in the river were investigated. The results show that the proposed model describes reasonably well the lithodynamic processes characteristic of fine flocculating sediments. Thus it seems possible to apply it for description of fine sediment transport under real wave–current conditions that occur in many marine waterbodies near river mouths.

Key words: SPM, flocculation, sediment transport model, turbulence

1. Introduction

Marine water is a very special and complicated mixture, whose composition has long been studied. Generally, it consists of pure water, dissolved matter and suspended particulate matter (SPM). The substances dissolved in seawater include all elements that occur in nature, namely gases, as well as numerous organic and inorganic compounds (Dera 2003), whereas SPM is composed of solids and gas bubbles. Inorganic suspension consists of fine sands and mineral particles of silt and mud fractions. Bigger particles that enter water have a very short life in suspension and settle rapidly. The basic components of inorganic marine suspension are quartz and clay minerals, such as illite, kaolinite, chlorite, montmorillonite and mixed-layer minerals (Rudziński 1986).

* This paper is dedicated to the memory of Professor Zbigniew Pruszak (1947–2018).

The distribution of suspension concentration is not equal in the world ocean. In addition, it changes over time. The highest concentrations are found close to river mouths and the polar regions during spring thaw (freshet). Spate and glacial waters carry enormous amounts of SPM to the sea at that time. Very high concentrations of SPM occur in the coastal zone. Noted values are up to hundreds of g m^{-3} (Bradtke 2004). The values of sediment concentration are lowest in the open sea and ocean far from land.

Inorganic particles that occur in seawater are mostly terrigenic. They reach the sea in three main ways: by river and glacial transport, through the atmosphere and by coast abrasion. River transport is the main source of mineral suspension in the sea. Inorganic matter enters rivers mainly as a result of riverbed erosion or is flushed from land surface by precipitation. The annual influx of mineral suspension to the world ocean by rivers is assessed at ca. 18.5 billion tons, which represents 13.2% of the total annual influx of SPM to the oceans (Bradtke 2004). Some researchers claim that farming and deforestation have doubled the total sediment yields over the last 2000–2500 years (Berner and Berner 1996). However, this increased sediment load is mitigated by dams (Geyer et al 2004).

The size range of suspension carried by a river depends on local hydrodynamic and hydrochemical conditions. Moreover, the amount of SPM transported by a river changes during the year. For example, rivers in polar and temperate zones are characterized by seasonal changes in water discharge, which are associated with variable SPM concentrations. The concentration of suspension delivered by a river to the sea is highest at the river mouth. That is also where the largest particles are observed. As the distance from the mouth increases, the SPM concentration and the content of the largest particles gradually decrease (Gurgul 1991).

Dusts of various kind are particles that enter seas through the atmosphere. They can be terrigenic, volcanic, cosmic or anthropogenic. Their estimated annual influx to the world ocean is approx. 4.1 billion tons, that is, ca. 2.9% of the total annual inflow of the suspension to the oceans (Bradtke 2004).

Inorganic matter also reaches the sea as a result of coast abrasion, that is, cliff, dune, beach and bottom erosion caused by waves and nearshore currents. This factor is of particular importance during storms, when strong waves and currents remove previously deposited material off shore (e.g. Ostrowski et al 2010, Szmytkiewicz and Zabuski 2017). Larger particles are deposited in the vicinity of the coast, but smaller one may remain suspended for a long time and reach the open sea. The estimated annual influx of mineral matter to the world ocean due to coast abrasion is about 0.5 billion tons, that is, 0.4% of the total annual influx of suspension to the oceans (Bradtke 2004).

Sediments are carried by sea currents, like the other components of marine water, and may be transported over significant distances, even thousands of kilometers. The vertical transport of SPM is generated by the settling of particles (sedimentation), the vertical component of the flow vector, and turbulent motions of water. Additionally,

in the coastal zone, an important role is played by the undulation of the sea. Thus, the resultant motion of particles is the consequence of the local circulation of water and the force of gravity. Its speed depends on the density, size and shape of particles. Therefore, the lifetime of sediments in suspension depends on many factors and can vary from a split second to thousands of years. Moreover, the sea bottom may be eroded, especially in the nearshore zone, which leads to the resuspension and subsequent redeposition of sediments. Thus, the presence of inorganic suspension in water is integrally connected with processes of coast and sea bottom formation. A mathematical model of the transport of suspended material may be a helpful instrument in a quantitative estimation of these processes.

The aim of this study is to present a theoretical description of the transport of suspended mineral material and to qualitatively assess its applicability in the modelling of fine sediment transport under real wave–current conditions in marine waterbodies near river mouths.

2. Flocculation of Fine Sediment

Flocculation is a very important process connected with fine suspension in the sea. It is a reversible process that results from the simultaneously occurring processes of aggregation of particles and floc break-up. It influences not only the size distribution of suspended particles, but also the transport of sediments and thereby the SPM concentration. This follows from the fact that aggregation is due to mutual collisions and subsequent adherence between particles of fine sediment. As a result, bigger and faster-sinking aggregates (flocs) are formed. Floc break-up is an antagonistic process in which single particles are torn off flocs and flocs are disintegrated into smaller aggregates.

Flocculation is governed by three factors: turbulence, Brownian motion and differential settling. However, many studies (e.g. McCave 1984, Stolzenbach and Elimelich 1994) show that the effects of Brownian motion and differential settling are negligible in coastal environments, so the effects of turbulence are dominant. Turbulent motion causes particles to collide and form flocs, but turbulent shear may disrupt flocs, causing floc break-up. This means that turbulence may either increase or decrease the size of flocs. Dyer (1989) showed that the mean floc size increases with shear rate, and after exceeding some threshold value, it decreases. Thus, aggregation dominates for small turbulent shear rates, whereas floc break-up processes dominate for higher values of the shear rate. Moreover, the floc size increases with increasing suspended sediment concentration.

Primary particles of suspension are multi-dispersive under natural conditions (clay, mud, sand particles), and floc sizes are very different as well. Their diameter may range from a few micrometers to a few millimeters (Curran et al 2007). Unfortunately, our knowledge about the process of flocculation is fraught with uncertainties – there are still many questions to answer. This makes it difficult to provide a reliable

description (model) of flocculation. Krone (1986) hypothesized that flocs are built hierarchically, forming an ordered structure. According to his conception, primary particles form first-order flocs by aggregation. These flocs come together, forming structures of the second order and so on. This is schematically depicted in Fig. 1.

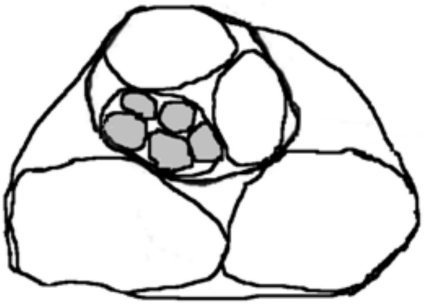

Fig. 1. Sketch of a hierarchical floc structure, modified after Krone (1986)

Treating flocs as fractal entities is a well-accepted approximation (Winterwerp 1999). The assumed self-similarity of flocs means that each arbitrary small piece of a floc is similar to a larger one. This approximation is somehow an extension of the conceptual order-of-aggregate description of flocs by Krone (1986). The concept of fractal dimension, which is a measure of the self-similarity of an object, is applied in this approach. The fractal dimension n_f is obtained from the description of a growing object having the linear size La and volume $V(La)$, where a is the linear size of the primary particle. It is assumed that $V(La)$ is proportional to $P(La)$, where P is the number of primary particles. Then, the fractal dimension n_f is defined as (Winterwerp 1999)

$$n_f = \lim_{L \to \infty} \frac{\ln (P\,(La))}{\ln (La)}. \tag{1}$$

The theoretical values of n_f can range from 1 (linear flocs) to 3 (spherical flocs). The lowest values are found for very fragile flocs, such as marine snow with $n_f \approx 1.4$ (Kranenburg 1994). Typical values in estuaries and coastal waters vary between $n_f \approx 1.7$ and 2.2, with an average of $n_f \approx 2.0$ (Winterwerp 1999). Smith and Friedrichs (2011) estimated the fractal dimension of flocs at 2.1–2.3. The higher values are associated with low mean velocities and high SPM concentrations (Dyer and Manning 1999) – for example, the fractal dimension of flocs in a fluid mud layer can be as large as $n_f \approx 2.6$–2.8 (Kranenburg 1994).

3. Model Description

The transport of sediments may be described by the advection-diffusion equation. However, this equation needs a certain modification: the settling velocity of SPM

has to be included. That is because the equation describes the transport of a passive substance, whereas SPM is not completely passive as it settles. The transport equation has the following form:

$$\frac{\partial c}{\partial t} + \frac{\partial (uc)}{\partial x} + \frac{\partial (vc)}{\partial y} + \frac{\partial ((w - w_S)c)}{\partial z} - K_H \frac{\partial^2 c}{\partial z^2} + \\ -A_H \frac{\partial^2 c}{\partial x^2} - A_H \frac{\partial^2 c}{\partial y^2} = 0, \tag{2}$$

where:

t	–	time,
c	–	SPM concentration,
w_S	–	settling velocity,
u, v, w	–	components of the velocity vector,
K_H and A_H	–	coefficients of vertical and horizontal turbulent diffusion.

The settling velocity is calculated from the formula (Winterwerp 1999)

$$w_s = \frac{\alpha}{18\beta} \frac{(\rho_s - \rho_w)\, g}{\mu} D_p^{3-n_f} \frac{D_f^{n_f - 1}}{1 + 0.15\, Re_f^{0.687}}, \tag{3}$$

where:

α, β	–	shape coefficients of flocs,
ρ_s	–	density of sediments (primary particles),
ρ_w	–	water density,
g	–	gravitational acceleration,
μ	–	dynamic viscosity of the fluid,
D_p	–	primary particle diameter,
D_f	–	floc diameter,
Re_f	–	Reynolds number for flocs.

Assuming that flocs are spherical ($\alpha = \beta = 1,\ n_f = 3$) and $Re_f \ll 1$, Eq. 3 would simplify to the commonly known Stokes formula.

Sediment transport through the water surface is equal to the sediment flux from the atmosphere. At the bed, flocs may enter or leave the domain through erosion or deposition processes. Hence the boundary conditions read as follows:

$$\left((w - w_s)\, c - K_H \frac{\partial c}{\partial z} \right) \Bigg|_{z=\eta} = \Theta_{atm,c}, \tag{4}$$

$$\left((w - w_s)\, c - K_H \frac{\partial c}{\partial z} \right) \Bigg|_{z=-h} = \Theta_{b,c}, \tag{5}$$

where:

η – free surface elevation,
h – bottom level,
$\Theta_{atm,c}$ – sediment flux from the atmosphere,
$\Theta_{b,c}$ – source-sink term.

The source-sink term $\Theta_{b,c}$ represents the exchange with the bed and is modeled by a commonly used formula of Partheniades-Krone:

$$\Theta_{b,c} = -w_s c H\left(s_d\right) + M H\left(s_e\right), \tag{6}$$

where:

M – bed erosion rate,
v_e – critical friction velocity for erosion,
v_d – critical friction velocity for deposition,
v_b – bottom friction velocity,
$H()$ – Heaviside function,

$$s_d = 1 - \frac{v_b^2}{v_d^2},$$
$$s_e = \frac{v_b^2}{v_e^2} - 1.$$

Fine sediments flocculate, so the phenomenon of flocculation should be taken into account. Therefore, the transport model is extended by a flocculation model of Winterwerp (1999). As there are many uncertainties, some simplifications have to be accepted. It is assumed that SPM consists of fine size-uniform sediments with the particle diameter D_p and all SPM is flocculated. In addition, all flocs in a unit volume have the same size. Then, the concept of the floc concentration N, which is the number of flocs per unit volume, is introduced by

$$N = \frac{1}{f_s} \frac{c}{\rho_s} D_p^{n_f - 3} D_f^{-n_f}, \tag{7}$$

where:

f_s – shape factor of flocs (e.g. for spherical objects, it equals $\pi/6$),

Flocculation is a dynamic process, and the floc concentration changes continuously. It follows from Eq. 7 that the floc concentration depends not only on the suspension concentration, but also on the floc diameter. That is why flocculation should be described regardless of the mass balance equation Eq. 2. Turbulence is the most favorable factor for flocculation in a marine environment, so it is assumed in the present

study that aggregation and floc break-up depend on turbulence only. The flocculation equation is given by Winterwerp (1999) as follows:

$$\frac{\partial N}{\partial t} + \frac{\partial (uN)}{\partial x} + \frac{\partial (vN)}{\partial y} + \frac{\partial ((w - w_x)N)}{\partial z} - K_H \frac{\partial^2 N}{\partial z^2} - A_H \frac{\partial^2 N}{\partial x^2} + \\ -A_H \frac{\partial^2 N}{\partial y^2} = -k'_A (1 - \Phi_*) G D_f^3 N^2 + k_B G^{q+1} \left(D_f - D_p\right)^p D_f^{2q} N, \tag{8}$$

where:

k'_A – efficiency coefficient for aggregation,

$\Phi_* = \min\{1,\ \Phi_f\}$,

Φ_f – volumetric concentration of flocs,
G – shear rate,
k_B – efficiency coefficient for floc break-up.

The left-hand side of Eq. 8 is the advection-diffusion term, while the right-hand side is the flocculation function. The first term on the right-hand side describes aggregation, and the second describes floc break-up processes. The volumetric concentration of flocs may be derived from Winterwerp (1999):

$$\Phi_f = f_s N D_f^3. \tag{9}$$

The shear rate is a measure of turbulence in the flow. It can be calculated using the turbulence model of Mellor and Yamada (1982) from the formula

$$G = \sqrt{\frac{\varepsilon}{\nu}} = \sqrt{\frac{q^3}{B_1 l \nu}}, \tag{10}$$

where:

ε – turbulent dissipation rate,
ν – kinematic viscosity of the fluid,
l – turbulence macroscale,
q^2 – turbulence kinetic energy,
B_1 – empirically determined constant.

The boundary conditions are consistent with those for mass balance (Eq. 4 and Eq. 5):

$$\left((w - w_s) N - K_H \frac{\partial N}{\partial z}\right)\Bigg|_{z=\eta} = \Theta_{atm,N}, \tag{11}$$

$$\left((w - w_s) N - K_H \frac{\partial N}{\partial z}\right)\Bigg|_{z=-h} = \Theta_{b,N}, \tag{12}$$

where:

$\Theta_{atm,N}$ – particle flux from the atmosphere,
$\Theta_{b,N}$ – source-sink term.

The particle flux from the atmosphere $\Theta_{atm,N}$ is calculated by Eq. 7, although only primary particles with the diameter D_p and sediment flux from the atmosphere $\Theta_{atm,c}$, instead of the sediment concentration c, are assumed. This yields the formula

$$\Theta_{atm,N} = \frac{\Theta_{atm,c}}{f_s \rho_s D_p^3}. \tag{13}$$

The source-sink term $\Theta_{b,N}$, representing floc exchange with the bed, is obtained in a similar way as Eq. 6 and takes the following form:

$$\Theta_{b,N} = -w_s N H(s_d) + \frac{M}{f_s D_{f,b}^3 \rho_{f,b}} H(s_e), \tag{14}$$

where:

$D_{f,b}$ – floc diameter on the bottom,
$\rho_{f,b}$ – floc density on the bottom.

Eq. 2 and Eq. 8 describe the transport of sediments and the process of flocculation. They are independent of each other, but consistent. It is important to distinguish the floc concentration from the SPM concentration (by mass), since these quantities have completely different meanings and they are also state variables in particular equations. All equations of the transport and flocculation models presented here have already been subjected to the classical Reynolds averaging procedure. This means that all variables are average variables in the Reynolds sense.

The transport of sediments is due to the interaction of marine currents and sedimentation, as well as wave motion in the nearshore region. Therefore, a hydrodynamic model is required to consider a complete transport model. Hydrodynamic equations provide information about current velocity and water density. These quantities are used in the sediment transport equations. The hydrodynamic model M3D (Kowalewski 1997) and a simple wave model are used in the present approach.

Wave motion plays a major role in hydrodynamic processes in the nearshore zone. Waves cause bed erosion and thus introduce bottom sediments into suspension. Here, a simplified wave model is included in the hydrodynamic model. The significant wave height H_S and the wave period T are given by (Young 1999)

$$H_S = 0.0016 \sqrt{L_f \frac{W^2}{g}}, \tag{15}$$

$$T = 0.2221 \left(\frac{L_f W}{g^2} \right)^{1/3}, \tag{16}$$

where:

L_f – wind fetch,
W – wind speed.

The maximal orbital velocity on the bottom at the depth h is given in a form valid for the linear wave theory, see e.g. (Weyhenmeier et al 1997):

$$U_0 = \frac{\pi H_S}{T \sinh\left(\frac{\pi h}{10 H_S}\right)}. \tag{17}$$

The bottom friction velocity is calculated according to (Danielsson et al 2007)

$$v_b = U_0 \sqrt{0.5 f_w}, \tag{18}$$

where the bottom friction coefficient f_w has the following form (Danielsson et al 2007):

$$f_w = \exp\left[5.5\left(\frac{A_b}{2.5 D_{f,b}}\right)^{-0.2} - 6.3\right], \tag{19}$$

where:

A_b – amplitude of orbital motion on the bottom.

The relationship between the orbital velocity and the amplitude of orbital motion can be expressed in the following form:

$$A = \frac{UT}{2\pi}, \tag{20}$$

where:

A – amplitude of orbital motion,
U – orbital velocity.

The amplitude of orbital motion on the bottom is obtained by substituting Eq. 17 into Eq. 20:

$$A_b = \frac{H_S}{2 \sinh\left(\frac{\pi h}{10 H_S}\right)}. \tag{21}$$

Near-bottom currents cause bed erosion in the offshore zone. The effect of waves is negligible there. The bottom friction velocity is given by

$$v_b = \sqrt{C_D} U, \quad C_D = \max\left\{\left(\frac{\kappa}{\ln \frac{\Delta z_b}{z_0}}\right)^2, 0.0025\right\}, \tag{22}$$

where:

C_D – drag coefficient,
U – near-bottom current velocity,
κ – von Karman constant,
z_0 – roughness parameter,
Δz_b – half of the bottom layer thickness.

The near-bottom current velocity U is taken from the M3D model. It is a three--dimensional baroclinic hydrodynamic model based on the ocean circulation model of Blumberg and Mellor (1987), known as POM (Princeton Ocean Model), which has been adapted by the Institute of Oceanography of Gdańsk University. See Kowalewski (1997) for a detailed description.

4. Model Setup

The model has been tested on a simplified waterbody, shown in Fig. 2. It is a bowl--shaped basin with a maximal depth of 50 m in the middle. Its latitudinal length is ca. 110 km (19°E–20°E), and its longitudinal length is ca. 60 km (59°N–60°N). The river mouth is located in the middle of the southern shore, whereas the open boundary is situated in the middle of the northern shore. It is assumed that sediments in the waterbody may originate from the river, the atmosphere and the eroding bed. The results of calculations obtained for the free surface, the bottom and two cross-sections: latitudinal AA′ and longitudinal BB′ (Fig. 2b) are analyzed.

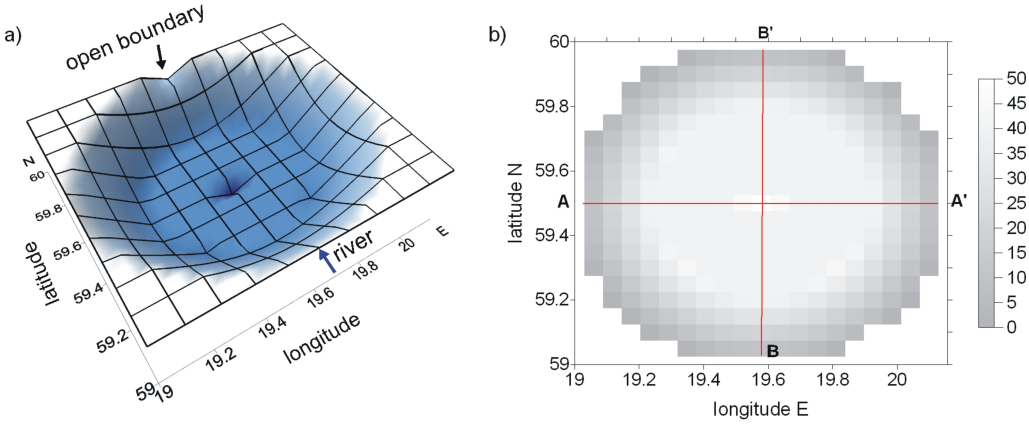

Fig. 2. Representation of the model design used for experiments: 3D view (a), top view with tagged cross-sections AA′ and BB′ (b)

The values of coefficients and parameters used in the model are given in Table 1.

The model was tested for several meteorological conditions, in particular for various wind directions and velocities. The values of wind parameters used in calculations

Table 1. The values of coefficients and parameters assumed in the model

coefficient	value
n_f [–]	2
q [–]	0.5
p [–]	1
k'_A [–]	0.31
k_B [$s^{0.5}$ m^{-2}]	14000

coefficient	value
f_s [–]	$\pi/6$
α [–]	1
β [–]	1
M [g m^{-2} s^{-1}]	$4 \cdot 10^{-5}$
ρ_s [g m^{-3}]	$2.65 \cdot 10^6$

coefficient	value
D_p [m]	$4 \cdot 10^{-6}$
v_d [m s^{-1}]	0.02
v_e [m s^{-1}]	0.03
$\Theta_{atm,c}$ [g $m^{-2}s^{-1}$]	$2.3 \cdot 10^{-6}$

are shown in Table 2. The western wind was not tested, because of the location of the river mouth, exactly in the middle of the southern coast, and the regular and symmetric shape of the basin. It is assumed that results for the western wind would be analogous to those for the eastern wind.

Table 2. Values of wind parameters

Wind direction	Wind speed [m s^{-1}]
N	5
S	5
E	5
E	10
E	15

The model was also tested for various discharges of fluvial sediments. Two parameters are considered in this case: river discharge and the fluvial SPM concentration. The values used in calculations are given in Table 3.

Table 3. Values of river discharge parameters

River discharge [m^3s^{-1}]	SPM concentration [g m^{-3}]
500	15
1000	15
1000	60

In addition, while testing the flocculation model some computations were also carried out in which flocculation was neglected. Such tests provided information about the influence of flocculation on bottom erosion, sediment deposition and the SPM concentration.

5. Exemplary Results

Please note that the results are shown in geographic coordinates, and the waterbody is oval. The computational results show higher waves in the vicinity of the leeward shore (Fig. 3). Bottom erosion is found in these areas, whereas deposition occurs in

the other parts of the waterbody (Fig. 4). The bottom erosion caused by the eastern wind is much smaller than that caused by northern and southern winds. In all cases, an area with increased deposition is located near the river mouth. The northern wind causes much greater sediment deposition close to the river mouth than do the eastern and southern winds.

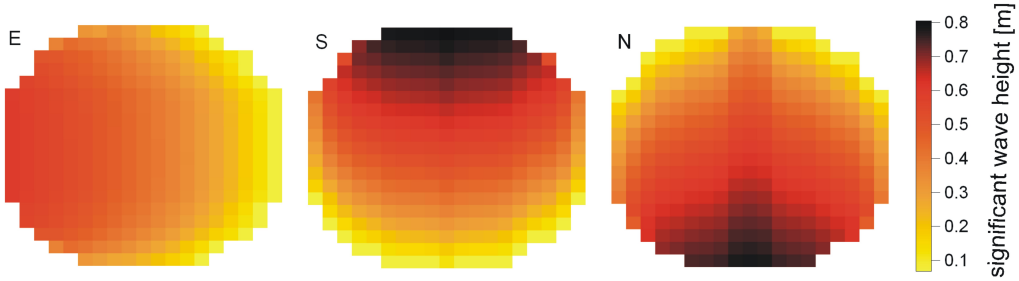

Fig. 3. Maps of the significant wave height for wind blowing from various directions at a speed of 5 m s^{-1}

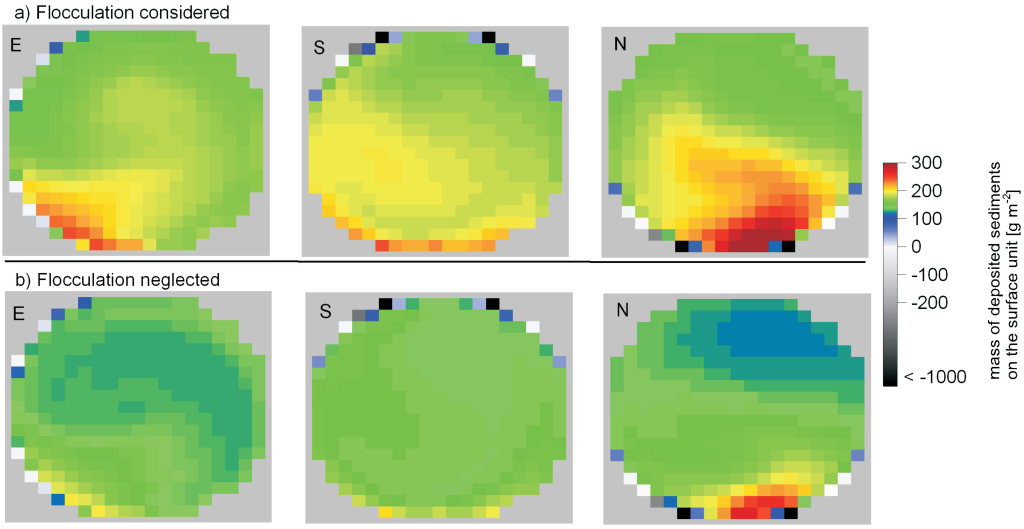

Fig. 4. Maps of bottom erosion and sediment deposition for winds blowing from various directions at a speed 5 m s^{-1}, a river discharge of 1000 m^3 s^{-1} and SPM concentration in the river of 15 g m^{-3}; flocculation considered (a), flocculation neglected (b)

When flocculation is neglected, the bottom erosion is similar as in the case in which it is considered (Fig. 4 and Fig. 5), but the deposition of sediments occurs more slowly. This is most evident near the river mouth and in the middle of the basin (Fig. 5).

Significant differences in the results occur for various wind speeds. An eastern wind blowing at a speed of 15 m s^{-1} causes intensive bottom erosion on the western

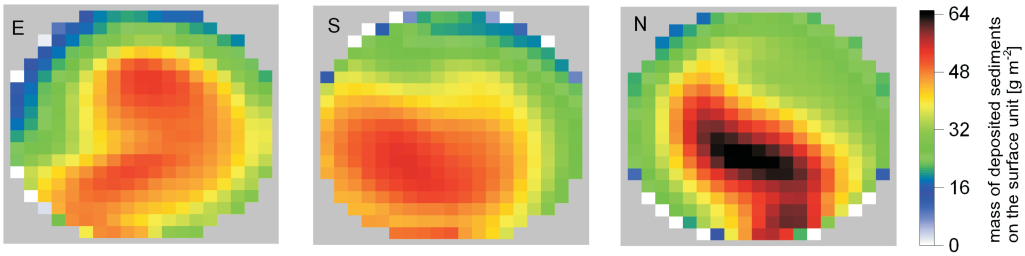

Fig. 5. Maps showing differences in bottom erosion and sediment deposition between cases with flocculation considered and neglected for winds blowing from various directions at a speed of 5 m s^{-1}, a river discharge of 1000 m^3 s^{-1} and SPM concentration in the river of 15 g m^{-3}

shore. Fast deposition of eroded material is observed in the vicinity of erosion areas at the same time (Fig. 6). The mass of sediments deposited in the other parts of the basin is much smaller.

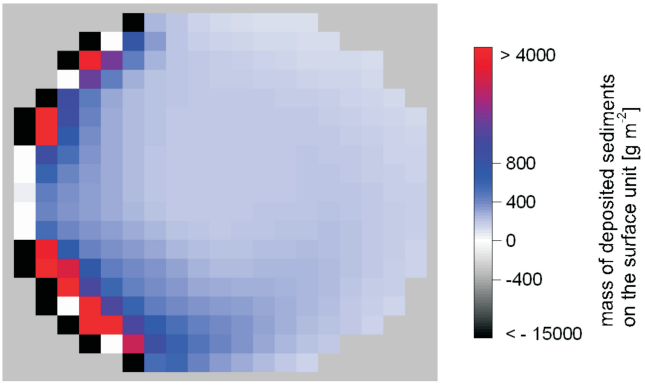

Fig. 6. Map of bottom erosion and sediment deposition for an eastern wind blowing at a speed of 15 m s^{-1} and no river discharge

A very high SPM concentration occurs on the western shore. It exceeds significantly the values of the SPM concentration in the rest of the basin. Floc diameters are also much bigger on the western shore than in the other parts of the waterbody. Additionally, they increase with depth (Figs. 7 and 8).

When flocculation is neglected, the SPM concentration in the whole basin is much higher than in the case in which flocculation is considered. The highest values are found on the western coast (Fig. 9). Moreover, the sediment concentration increases with depth.

The results for an eastern wind blowing at a speed of 10 m s^{-1} show intensive bottom erosion on the western shore. However, the amount of eroded material is noticeably smaller than in the case of wind blowing at a speed of 15 m s^{-1} (Fig. 10). Deposition of sediments is slightly greater in the vicinity of erosion areas than in the

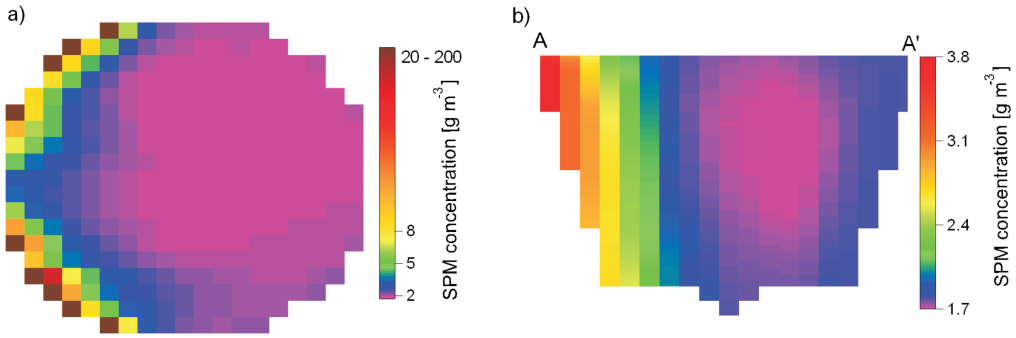

Fig. 7. The SPM concentration distribution on the free surface (a) and the latitudinal cross-section AA′ (b) for an eastern wind blowing at a speed of 15 m s^{-1} and no river discharge

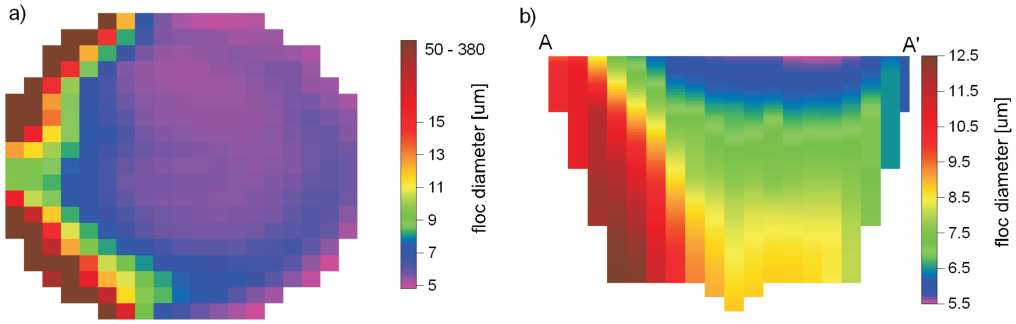

Fig. 8. The floc size distribution on the free surface (a) and the latitudinal cross-section AA′ (b) for an eastern wind blowing at a speed of 15 m s^{-1} and no river discharge

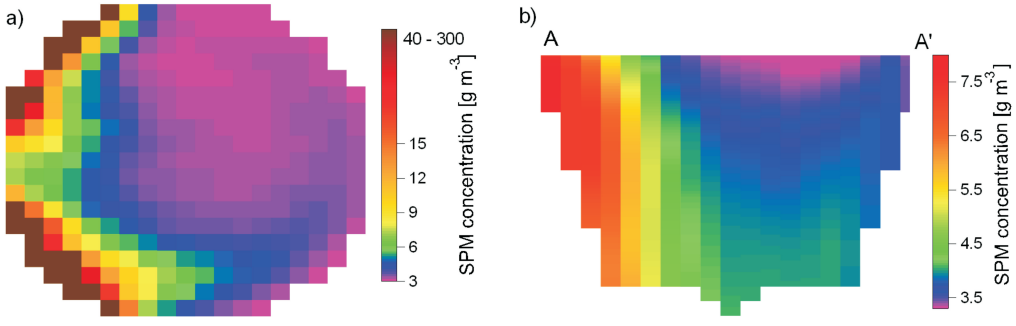

Fig. 9. The SPM concentration distribution on the free surface (a) and the latitudinal cross-section AA′ (b) for an eastern wind blowing at a speed of 15 m s^{-1}, no river discharge and no flocculation

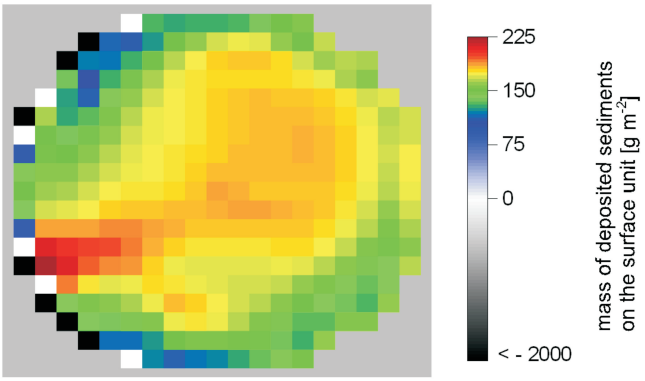

Fig. 10. Map of bottom erosion and sediment deposition for eastern wind blowing at a speed of 10 m s^{-1} and no river discharge

rest of the basin. The mass of sediments deposited in the remaining part of the basin is similar to that obtained for wind blowing at a speed of 15 m s^{-1}.

An area with a higher SPM concentration occurs on the western shore, although the difference between concentrations in this area and the rest of the basin is quite small. This area is funnel-shaped and extends into the middle of the basin (Fig. 11a). Almost no variation occurs in the SPM concentration in the vertical. Changes are slight also along the latitudinal cross-section AA′, that is, along the wind direction. The highest values are found on the western shore (Fig. 11b).

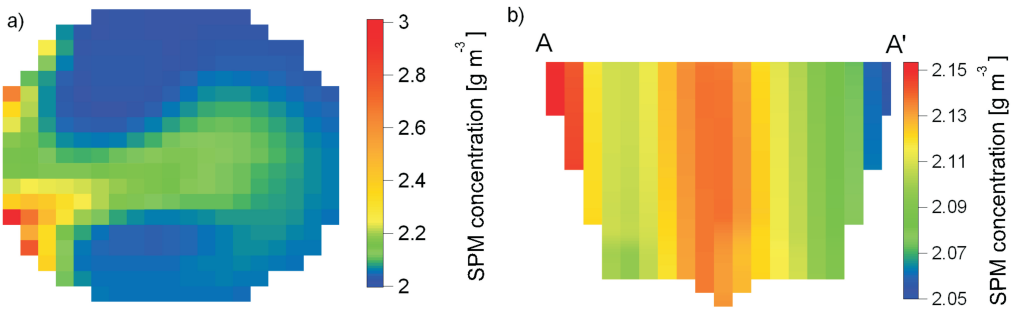

Fig. 11. The SPM concentration distribution on the free surface (a) and the latitudinal cross-section AA′ (b) for an eastern wind blowing at a speed of 10 m s^{-1} and no river discharge

The largest floc diameters occur in the erosive area on the western shore. Additionally, an increase in floc sizes is observed in the middle of the southeastern part of the waterbody. The area with bigger flocs is mushroom-shaped, with a stem based on the western shore (Fig. 12a). There is almost no variation in the floc diameter in the vertical, whereas some differences appear along the latitudinal cross-section. Floc sizes increase from the coast towards the middle of the waterbody (Fig. 12b).

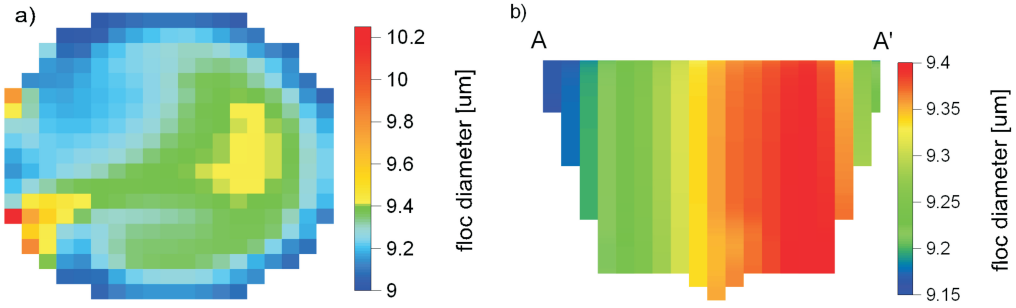

Fig. 12. The floc size distribution on the free surface (a) and the latitudinal cross-section AA′ (b) for an eastern wind blowing at a speed of 10 m s^{-1} and no river discharge

In the case of an eastern wind blowing at a speed of 5 m s^{-1}, the deposition of sediments takes place at a similar rate almost in the whole basin. A significant decrease in the deposition rate is observed only on the western coast (Fig. 13). However, it is a hindered deposition rather than bottom erosion that occurs in this area. Therefore, this case is completely different from those with larger wind speeds.

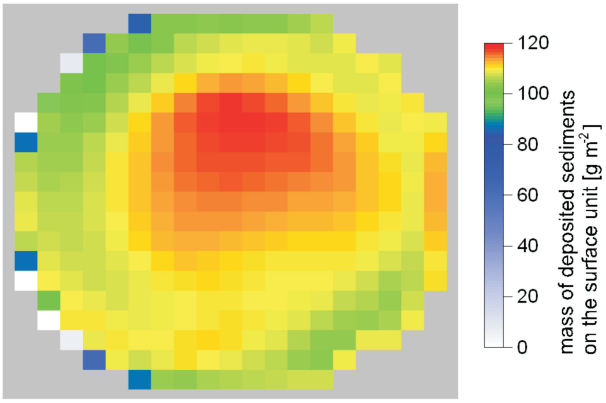

Fig. 13. Map of bottom erosion and sediment deposition for an eastern wind blowing at a speed of 5 m s^{-1} and no river discharge

A slight increase in the SPM concentration is observed on the western shore in comparison with the rest of the basin (Fig. 14a). Despite the fact that the differences are of the order of magnitude of 10^{-2} g m^{-3}, an analogy to cases with larger wind speeds occurs there. Some diversity is observed in the distribution of the SPM concentration in the vertical and along the wind direction. A lower SPM concentration occurs near the bottom and eastwards (Fig. 14b).

For floc sizes, the situation is the opposite. Flocs are slightly smaller on the western coast at this time (Fig. 15a). Some diversity is also observed in the vertical floc size distribution: slightly larger flocs occur near the bottom (Fig. 15b).

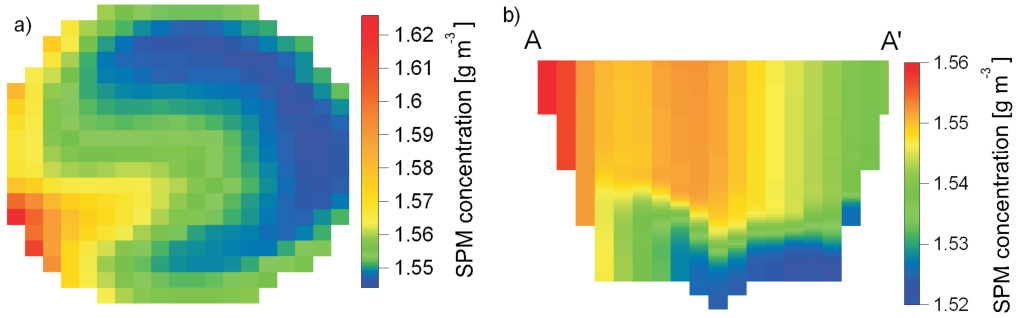

Fig. 14. The SPM concentration distribution on the free surface (a) and the latitudinal cross-section AA′ (b) for an eastern wind blowing at a speed of 5 m s^{-1} and no river discharge

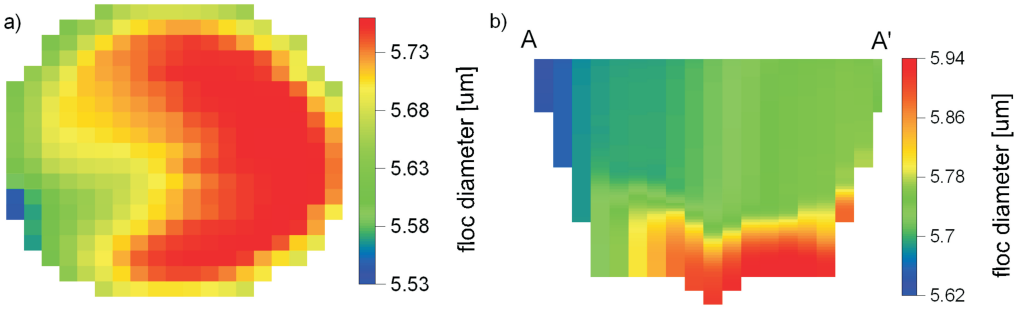

Fig. 15. The floc size distribution on the free surface (a) and the latitudinal cross-section AA′ (b) for an eastern wind blowing at a speed of 5 m s^{-1} and no river discharge

Each river carries some suspended sediments, so while flowing into a waterbody, it changes suspension dynamics and affects equilibrium conditions. Three river discharge cases were tested in the present study. A river discharge of 1000 m^3s^{-1} with SPM concentration of 15 g m^{-3} was considered as a benchmark (Table 3). This case is called a "standard river" in the present tests.

In the case of the standard river, the deposition of sediments is greater than it is for a river discharge of 500 m^3s^{-1} because of the larger suspension influx to the waterbody. In both cases, the largest deposition occurs near the river mouth. Sedimentary structures formed as a result of deposition are also similar. They differ only in the mass of sediments deposited (Fig. 16 a, b). The layouts of the distribution of the SPM concentration on the free surface and along the longitudinal cross-section BB' are also similar. However, higher concentrations are observed in the waterbody near the standard river. In both cases, the SPM concentration is highest near the river mouth. As the distance from the mouth increases, the SPM concentration decreases gradually. The value of the SPM concentration decreases also with increasing depth (Fig. 16 c–f).

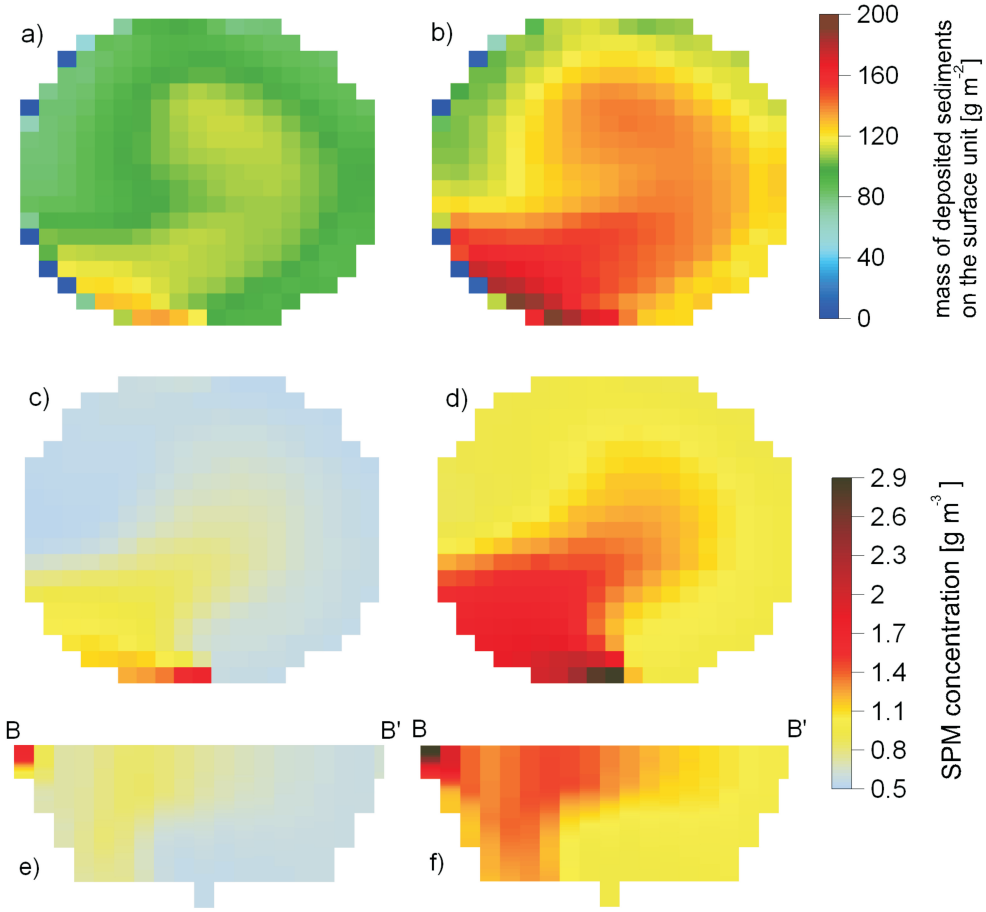

Fig. 16. A comparison of model results obtained for a river discharge of 500 m^3 s^{-1} (left) with results obtained for a river discharge of 1000 m^3 s^{-1} (right): a map of bottom erosion and sediment deposition (a and b), the distribution of the SPM concentration on the free surface (c and d) and the distribution of the SPM concentration along the longitudinal cross-section BB′ (e and f); SPM concentration in the river of 15 g m^{-3}, an eastern wind blowing at a speed of 5 m s^{-1}

Similar remarks can be made while comparing the results for the standard river case with those obtained for the river with SPM concentration of 60 g m^{-3}. For the river with a higher SPM concentration, deposition is greater because of the larger sediment influx to the waterbody (Fig. 17 a, b). Similar observations apply to the distributions of the SPM concentration on the free surface and along the longitudinal cross-section BB'. Higher concentration values are observed in the waterbody near the river with a higher SPM concentration. In both cases, the highest SPM concentration and the largest sediment deposition occur close to the river mouth. The SPM concentration diminishes gradually as the distance offshore from the mouth increases. The SPM concentration decreases also with increasing depth (Fig. 17 c–f).

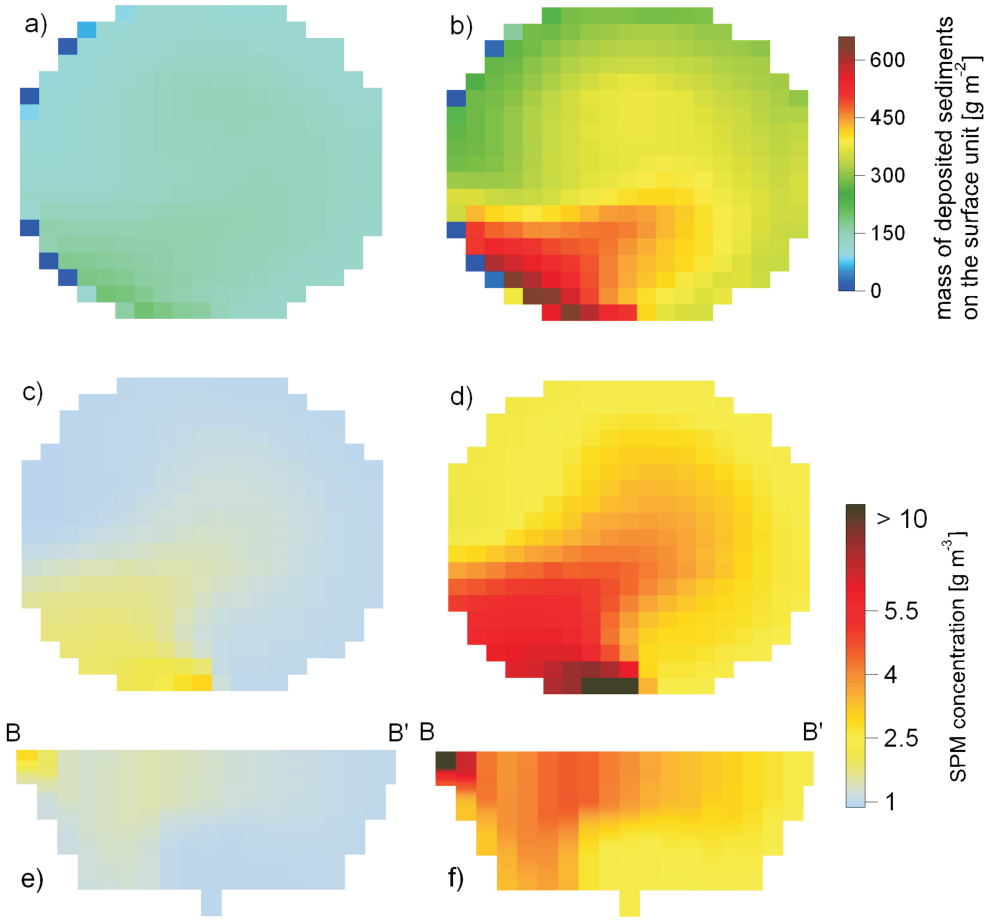

Fig. 17. A comparison of model results obtained for a river with SPM concentration of 15 g m^{-3} (left) with results obtained for a river with SPM concentration of 60 g m^{-3} (right): the map of bottom erosion and sediment deposition (a and b), the distribution of the SPM concentration on the free surface (c and d) and the distribution of the SPM concentration along the longitudinal cross-section BB′ (e and f); a river discharge of 1000 m^3 s^{-1}, an eastern wind blowing at a speed of 5 m s^{-1}

6. Conclusions

The computational simulations indicate that bottom erosion is due to the impact of high waves in shallow water on the leeward shore. The bottom erosion rates caused by the northern and southern winds blowing at a speed of 5 m s^{-1} are similar, while the eastern wind blowing at the same velocity causes only slight sedimentation on the western shore. This disproportion is due to the fact that the latitudinal fetch is about 110 km, while the longitudinal fetch is only about 60 km. That is why waves occurring on the southern and northern shores are higher than those on the western shore. Flocculation does not affect bottom erosion.

The results show that the increase in the SPM concentration due to bottom erosion accelerates flocculation because it facilitates the formation of bigger flocs. Therefore, in areas where strong bottom erosion occurs, larger flocs are observed. Due to undertow action, these flocs are transported inwards the basin, where they are deposited on the bottom. This finding is especially well supported by model calculations for a strong wind blowing at a speed of 15 m s^{-1}. The smaller the flocs, the slower they settle and the further away from the coast the current carries them. This effect of the undertow is more evident in the case of an intermediate wind blowing at a speed of 10 m s^{-1}. Flocs are transported further and then deposited.

No bottom erosion is predicted by the model for an eastern wind blowing at a speed of 5 m s^{-1}, but a slight decrease in floc size is noted on the leeward shore. This is probably due to the shear stress and the absence of sediment influx from bottom erosion. In the case of stronger winds, bottom erosion and a significant increase in the SPM concentration are found, so flocculation occurs in spite of the shear stress.

Increased deposition is observed westward of the river mouth in the case of the eastern wind. The southern wind causes an outflow of river waters to the north, and therefore the model calculations show a slightly increased deposition of sediments in a wide area in the southern part of the waterbody. The biggest amounts of sediment are deposited in the case of the northern wind. This is explained by two independent concurrent phenomena: the river discharge and the bottom erosion on the southern coast due to the northern wind. If no flocculation is assumed, sediment deposition decreases. In this case, the whole suspension consists of small particles, which settle more slowly than flocs. This leads to a significant increase in the SPM concentration in the whole basin.

An increase in the SPM concentration in the vicinity of the river mouth is an obvious consequence of the river discharge assumption. It is present even in the case of a strong crosswind. The SPM concentration decreases as the distance from the mouth increases, although it occurs more slowly in the direction of the wind.

The results show that the present model provides a reasonably good description of lithodynamic processes characteristic of fine flocculating sediments. Thus it seems possible, after further improvements, to apply this model for description of fine sediment transport under real wave–current conditions that can be found in many marine waterbodies in the vicinity of river mouths.

Acknowledgments

The authors wish to thank Prof. Rafał Ostrowski for valuable discussions on the manuscript.

References

Berner E. K., Berner R. A. (1987) *The Global water Cycle: Geochemistry and Environment*, Prentice-Hall, Englwood Cliffs, New Jersey, 397 p.

Blumberg A. F., Mellor G. L. (1987) A description of the three-dimensional coastal ocean circulation model, [in:] *Three-Dimensional Coastal Ocean Models*, N. Heaps (Ed.), Am. Geoph. Union, 1–16.

Bradtke K. (2004) *The suspension field and its influence on optical properties of coastal waters (Gdansk Bay, Baltic Sea)*, Ph.D. Thesis, Department of Physical Oceanography, Institute of Oceanography, Gdańsk University, Gdynia, 173 p. (in Polish).

Curran K. J., Hill P. S., Milligan T. G., Mikkelsen O. A., Law B. A., Durrieu de Madron X., Bourrin F. (2007) Settling velocity, effective density, and mass composition of suspended sediment in a coastal bottom boundary layer, Gulf of Lions, France, *Continental Shelf Research*, **27**, 1408–1421.

Danielsson Å., Jönsson A., Rahm L. (2007) Resuspension patterns in the Baltic proper, *Journal of Sea Research*, **57**, 257–269.

Dera J. (2003) *Marine physics*, PWN, Warszawa, 541 p. (in Polish).

Dyer K. R. (1989) Sediment processes in estuaries: future research requirements, *Journal of Geophysical Research*, **94** (C10), 14327–14339.

Dyer K. R., Manning A. J. (1999) Observation of the size, settling velocity and effective density of flocs, and their fractal dimensions, *Journal of Sea Research*, **41**, 87–95.

Geyer W. R., Hill P. S., Kineke G. C. (2004) The transport, transformation and dispersal of sediment by buoyant coastal flows, *Continental Shelf Research*, **24**, 927–949.

Gurgul H. (1991) *The dispersive systems in the sea*, Wyd. Nauk. Uniwersytetu Szczecińskiego, Szczecin, 248 p. (in Polish).

Kowalewski M. (1997) A three-dimensional hydrodynamic model of the Gulf of Gdansk, *Oceanological Studies*, **26** (4), 77–98.

Kranenburg C. (1994) The fractal structure of cohesive sediment aggregates, *Estuarine, Coastal and Shelf Science*, **39** (5), 451–460.

Krone R. B. (1986) The significance of aggregate properties to transport processes, *Proceedings of a Workshop on Cohesive Sediment Dynamics with Special Reference to Physical Processes in Estuaries*, Tampa, Florida, Springer Verlag, Coastal and Estuarine Studies, 14, 66–84.

McCave I. N. (1984) Size spectra and aggregation of suspended particles in the deep ocean, *Deep Sea Research*, **31** (4), 329–352.

Mellor G. L., Yamada T. (1982) Development of a turbulent closure model for geophysical fluid problems, *Rev. Geophys.*, **20**, 851–875.

Ostrowski R., Pruszak Z., Skaja M., Szmytkiewicz M., Trifonova E., Keremedchiev S., Andreeva N. (2010) Hydrodynamics and lithodynamics of dissipative and reflective shores in view of field investigations, *Archives of Hydro-Engineering and Environmental Mechanics*, **57** (3–4), 219–241.

Rudziński W. (1986) *The mineral suspension content in Gdansk Bay waters (Vistula mouth)*, M.Sc. Thesis, Institute of Oceanography, Gdańsk University, Gdynia, 64 p. (in Polish).

Smith S. J., Friedrichs C. T. (2011) Size and settling velocities of cohesive flocs and suspended sediment aggregates in a trailing suction hopper dredge plume, *Continental Shelf Research*, **10**, S50–S63.

Stolzenbach K. B., Elimelich M. (1994) The effect of density on collisions between sinking particles: implications for particle aggregation in the ocean, *Journal of Deep Sea Research I*, **41** (3), 469–483.

Szmytkiewicz P., Zabuski L. (2017) Analysis of dune erosion on the coast of south Baltic Sea with taking into account dune landslide processes, *Archives of Hydro-Engineering and Environmental Mechanics*, **64** (1), 3–15.

Weyhenmeier G. A., Hakanson L., Meili M. (1997) A validated model for daily variations in the flux, origin, and distribution of settling particles within lakes, *Limnol. Oceanogr.*, **42** (7), 1517–1529.

Winterwerp J. C. (1999) *On the dynamics of high-concentrated mud suspensions*, Ph.D. Thesis, Delft University of Technology, Delft, 172 p.

Young I. R. (1999) *Wind generated ocean waves*, Elsevier, 83 p.